# Numerical investigations of centrifugal compressor with corrosion pit defect preset on the disk and blade

**†S. Y. Chen, Y. P. Qu, X. X. Tang, D. D. Wan and J. Y. Pan**

Key Laboratory of High-efficiency and Clean Mechanical Manufacture, School of Mechanical Engineering, Shandong University, Jinan, Shandong, 250062, P. R. China

†Corresponding author: chensy66@sdu.edu.cn

**Abstract**

Three dimensional numerical investigations of a centrifugal compressor with pitting corrosion defect preset on the disk and blade are presented by FLUENT software. The pitting defect parameters such as the velocity field and pressure distribution in the gas passage are analyzed. With that purpose, the RNG k-ε two−equation turbulence model and simple algorithm are used based on the Navier-Stokes equation. Meanwhile, the DPM model is used to simulate the second phase particles deposit around the pitting corrosion defect. The chosen model provides a reference for the compressor impeller material stress corrosion test. The simulation results showed that the velocity gradient and static pressure decreased sharply while dynamic pressure increased and the chloride concentration was 50 times higher than before in the pitting area. The results could be as guidance for compressor serving in nature gas containing chloride ion to estimate the importance of ion concentration in the stress corrosion originated pitting defect.

**Key words:** centrifugal compressor, impeller, numerical simulation, pitting corrosion defect

## 1 Introduction

With respect to a compressor, the service life mainly depends on integrity and safety of the impellers. It is very difficult to do theoretical and experimental studies in fluid flow inside the impeller. Lots of researchers investigate the flow peculiarity inner the compressor without minor damage in the gas passage. The velocity and pressure changes due to minor defect such as pitting and micro cracks in the impeller will influence the generation and extension of cracks which affecting the performance and operation security of a centrifugal compressor. The crack propagation on the blade surface will lead to efficiency droop and abnormal vibrations. Numerical investigation on the compressor performance with defect on the blade is of alternative important to determine the velocity and pressure redistribution [1].

The turbulence model method is widely used for solving viscous flow in recent years. The k-ε two-equation model has reached success in engineering application for its own clear physical background [2]. The standard k-ε model is widely used in the centrifugal compressor impeller. However, the standard k-ε model has great restriction for that in the analysis of internal flow impeller machinery ignoring the anisotropy of turbulence. For that reasons, the standard k-ε model is only suitable for predicting simple isotropic turbulence [3-4]. In 1986, Yakhot and Orzag [5] came up with the dynamic renormalization group (RNG) k-ε model for the first time and the model allows us to evaluate transport coefficients and transport equations for the large-scale transport modes. The k equation and ε equation are as follows:

$$\frac{\partial(\rho k)}{\partial t}+\frac{\partial(\rho k u_i)}{\partial x_i}=\frac{\partial}{\partial x_j}\left[\alpha_k \mu_{eff}\frac{\partial k}{\partial x_j}\right]+G_k+\rho\varepsilon \tag{1}$$

$$\frac{\partial(\rho\varepsilon)}{\partial t}+\frac{\partial(\rho\varepsilon u_i)}{\partial x_i}=\frac{\partial}{\partial x_j}\left[\alpha_\varepsilon \mu_{eff}\frac{\partial k}{\partial x_j}\right]+\frac{c_{1\varepsilon}^{*}\varepsilon}{k}-G_{2\varepsilon}\rho\varepsilon\frac{\varepsilon^2}{k} \tag{2}$$

Where $\alpha_k$, $\alpha_z$ are the Prandtl numbers. $G_k$ is turbulence kinetic energy generated by laminar velocity gradient, k is turbulence kinetic energy, $\mu_{eff}$ is eddy viscosity, $\varepsilon$ is dissipation term.

Compared with the standard k–ε equation, the RNG k-ε equation takes the average flow in rotational flow. Based on the k–ε equation, it adds an item which reflects the strain rate of the mainstream. The RNG k-ε model is not only related with the flow movement, but also a function in spatial coordinates. So, it is easier to manipulate the high strain rate and large gradient of streamlining curvature.

Shengbo[6] discovered that different k-ε models calculation results varied widely in the simulation of the centrifugal compressor impeller. RNG k-ε model can be used to study the separation movement of the blade suction surface while standard k-ε and Realizable k-ε cannot. The RNG k-ε model can be used to not only simulates a wide range of separation vortex, but also distinguish the nuances of small-scale vortex structure. For this reason, the researchers give priority to use the RNG k-ε model in the flow simulation of centrifugal compressor impeller [7-8]. Before 1980s, inviscid flow simulation is adopted because of the limitation of hardware. Zhonghua Wu proposed the theory of S1/ S2 streaming surface, and Li [9] successfully carried out a simulation of impeller inner flow field to display the motion in average S2 stream surface. In the stage of inviscid simulation, quasi-orthogonal calculation also played an important role in numerical simulation [10]. In1980-1990, the researchers took viscosity of the fluid, backflow and eddy influence into consideration. In the period, many computational methods were adopted. Epureanu [11] simulated the impeller inner fluid with inviscid-viscous turbulence model, potential function calculated inviscid part while integral for viscous part. Gang Zhu carried the impellor inner fluid simulation with vorticity-steam function method in viscous fluid condition. Borello [12] put up with the finite element overlap base on the development of computer with high configuration and parallel computing technique.

The paper focuses on the compressor impeller in natural gas transportation project to explore the influences of chloride abundant that could lead stress corrosion. It can be the guidance of preventative maintenance and security operating.

## 2 Numerical analysis method

The compressor works at a constant angular speed. The control equations for the system are Navier-Stokes equation, continuity equation and energy equation in a relatively cylindrical coordinate system. The calculation solver is Pressure-Based type coupled implicit solver. The turbulence model is RNG k-ε model and the coupled of velocity and pressure is SIMPLE. Computed variables adopted the second order upwind format and residual error is $10^{-3}$ convergence. The second phase particle $Cl^-$ will be added from the inlet of the impeller with 2 percent of the compressor mass-flow after the calculation completed. The control parameters are that the time step is 1 *ms*, calculation steps are 5000 with unsteady particle tracking. The particle injects into continuous phase each iteration step 30. The simulation is based on steady-state.

Navier-Stokes equation:

$$\frac{Du_i}{Dt} = f_i - \frac{1}{\rho}\frac{\partial p}{\partial x_i} + v\nabla^2 u_i + \frac{1}{3}v\nabla(\nabla u_i) \tag{3}$$

Continuity equation:

$$\frac{\partial \rho}{\partial t} + \nabla \cdot (\rho u_i) = 0 \tag{4}$$

Gas state equation:

$$p = \rho RT \tag{5}$$

Energy equation:

$$\frac{\partial(\rho T)}{\partial t} + \mathrm{div}(\rho u_i t) = \mathrm{div}(\frac{k}{c_p}\,\mathrm{grad}T) + S_T \tag{6}$$

Particle trajectory control equation:

$$\frac{du_i^p}{dt} = F_D + F_g + F_B + F_L + F_T \tag{7}$$

Particle stokes law FD expression for resistance equation:

$$F_D = \frac{18\mu}{d_p^2 \rho_p c_c}(\mu_i - \mu_i^p) \tag{8}$$

Thermophoresis force FT expression equation:

$$F_T = -D_T \frac{1}{m_p T}\frac{\partial T}{\partial x} \tag{9}$$

Where $\mu$ is the kinematic viscosity, $\rho$ is the density, t is time, $u_i$ is the velocity, R is molar gas constant, Cp is specific heat capacity, T is temperature and k is heat transfer coefficient and the $S_T$ is the internal heat source. Cc is slip coefficient, Fg is gravity, $F_B$ is brown power, $\Delta t$ is time step, $S_0$ is spectral intensity function, $F_L$ is Saffman lift force and $D_T$ is the swimming thermal coefficient.

## 3 Analysis model and the grid

### 3.1 *Boundary conditions*

The numerical simulation model is the stage 2 impeller containing 11 long blades and 11 short blades. The circumferential velocity of compressor is 296.9 *m/s* and the inlet pressure is 0.17 *MPa*. The outlet diameter is 918 *mm*. The inlet temperature is 350 *K*. The mass-flow of the impeller is 26 *Kg/s* with compression ratio 4:1. The impeller geometric 3-D model and flow channels 3-D model are shown in Figure 1.

In the outlet, pressure-outlet is taken as boundary condition..

**Figure 1. Impeller geometric model and flow channels model.**

### *3.2 Grid*

As shown in Table 1, the static pressure and total pressure extracted on the pitch-averaged surface would keep steady with the increase of mesh number. The Tet/Hybrid mixed grid type is used to mesh flow channel with 2642992. The mesh is shown in Figure 2.

The pitting is taken as the first step of the stress corrosion where the micro-cracks appear. The flow field pressure changes and distribution of corrosion ion plays a vital role in crack initiation and propagation. In order to examine the influential factors of stress corrosion in crack initiation and propagation, two corrosion pit defects of 2 *mm* in diameter on the disk and pressure surface are preset for simulating the flow field of impeller, respectively.

**Table 1. Test for grid independence**

| Mesh number | Static pressure /MPa | Total pressure /MPa |
|---|---|---|
| 1506543 | 0.1366 | 0.1898 |
| 2642992 | 0.1366 | 0.1798 |
| 3207642 | 0.1366 | 0.1775 |

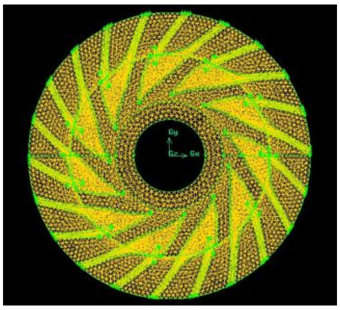

**Figure 2. The sketch mesh of flow channel model.**

The grid of pitting corrosion defect on disk and blade are refined as 63 and 106, respectively, as shown in Figure 4.

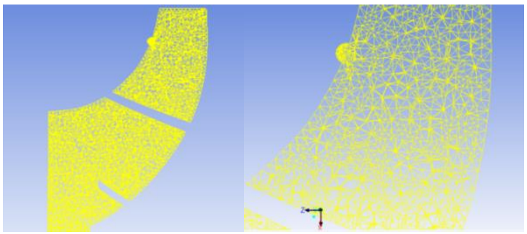

**Figure 3. The grid of pitting on disk**

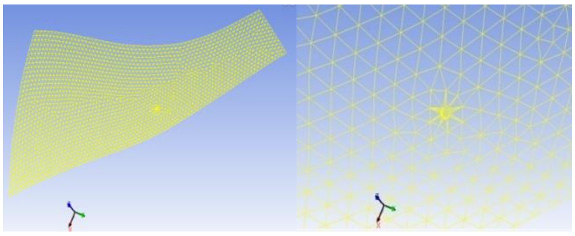

**Figure 4. The grid of pitting on blade**

## 4 Simulation results and analysis

### 4.1 *Pressure and velocity distribution of impeller*

According to the distribution of static pressure and total pressure of the impeller showed in Figure 5. In the inlet of the blade, there is significant low pressure area and pressure gradient at the head of the blade. Velocity distribution is seen in Figure 6.

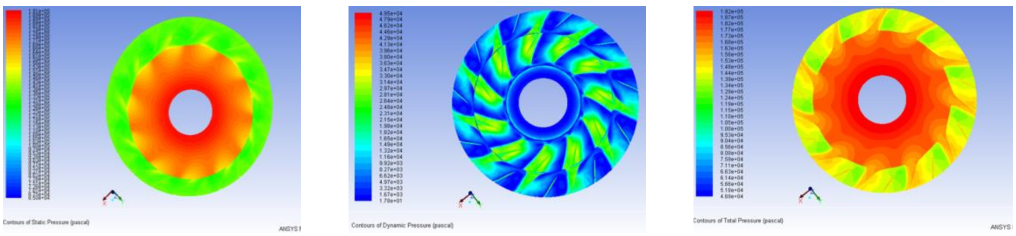

(a) static pressure (b) dynamic pressure （c） total pressure

**Figure 5. The pressure distribution of the impeller**

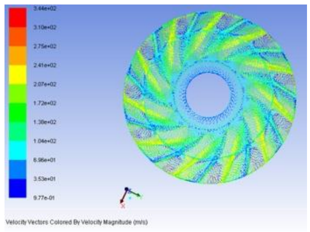

**Figure 6. The velocity vector of the impeller**

4.2 *Pressure, velocity and corrosion ion distribution at the corrosion pit defect of the disk*

As shown in Figure 7 and 8, static pressure increases and dynamic pressure reduces quickly in the incident surface of pitting defect. The velocity and velocity gradient decrease sharply and backflow vortex appears in pitting in which the static pressure decreased while dynamic pressure increased. There are a large number of backflow eddies especially in the passage of impeller according to Figure 9 and 10.

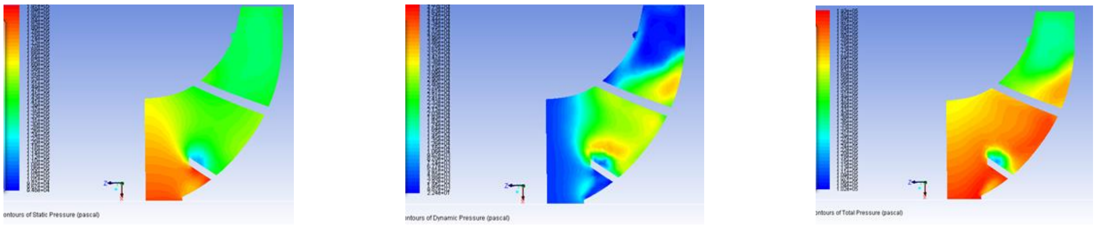

(a) static pressure in passage (b) dynamic pressure in passage (c) total pressure in passage

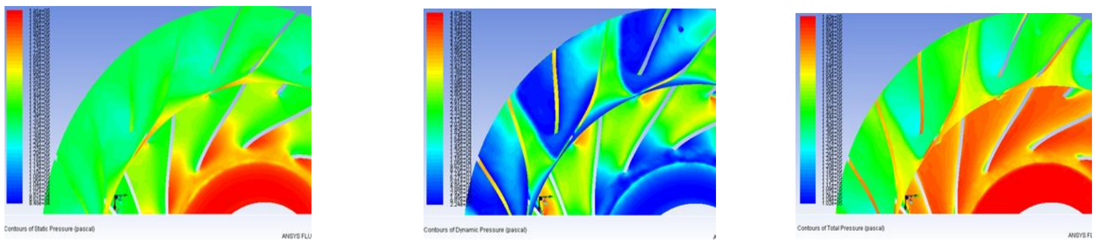

(d) static pressure on disk (e) dynamic pressure on disk (f) total pressure on disk

**Figure 7. The pressure distribution of the passage and disk**

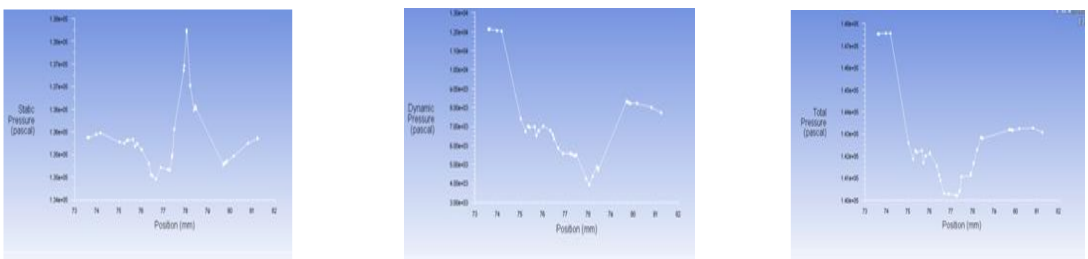

（a） static pressure (b) dynamic pressure (c) total pressure

**Figure 8. The pressure distribution on the corrosion pit defect of the disk**

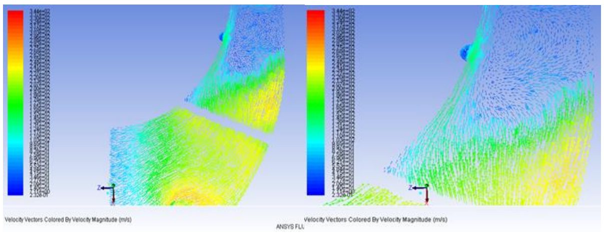

**Figure 9. The velocity vector on the pit defect of the disk**

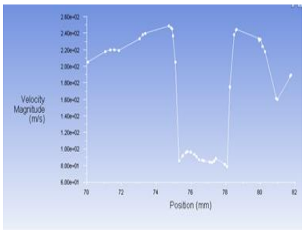


**Figure 10. The velocity distribution on the of the disk**

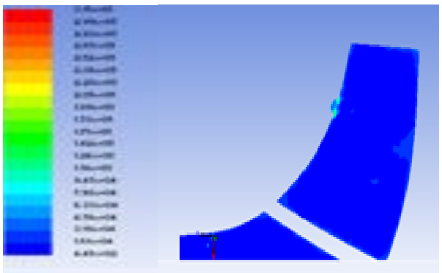

**Figure 11. The strain rate on the pit of the disk**

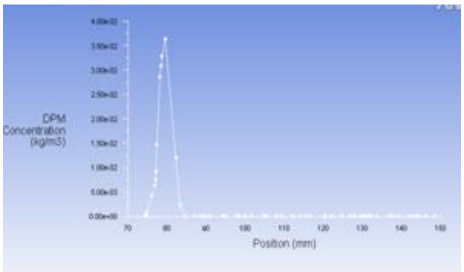


**Figure 12. The sedimentary concentration of Cl- at pit of the disk**

The flow strain rate at the pitting defect of the disk changes considerably as shown in Figure 11. The sedimentary concentration at the pitting defect of the disk is shown in Figure 12. It is found that the Cl- concentration is 50 times higher than before in the pitting area. The pitting defect area should be easy to be the origin of the crack because the Cl- is reactive ion to the corrosion of high strength stainless steel. The deduction can be further proved by the fact that the results of simulation coinciding with the stress corrosion test.

*4.3 Pressure, velocity and corrosion ion distribution at the corrosion pit defect of the blade*

The static pressure increases in the incident surface of pitting defects and dynamic pressure reduces quickly as shown in Figure 13, 14, 15 and Figure 16. The static pressure reduces and dynamic pressure increase in pitting defect. Fluid strain rate on the pitting defect of the blade changes considerably as shown in Figure 17, 18 and19.

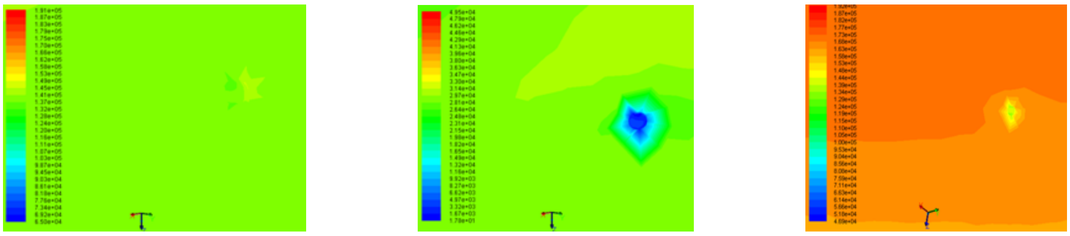

(a) static pressure (b) dynamic pressure (c) total pressure

**Figure 13. The pressure at corrosion pit of the blade**

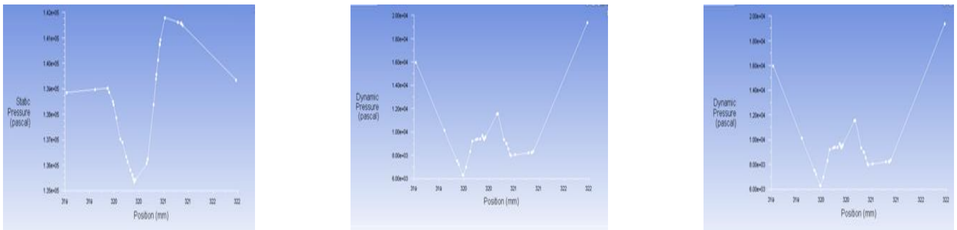

(a) static pressure (b) dynamic pressure (c) total pressure

**Figure 14. The pressure distribution curve at pit of the blade**

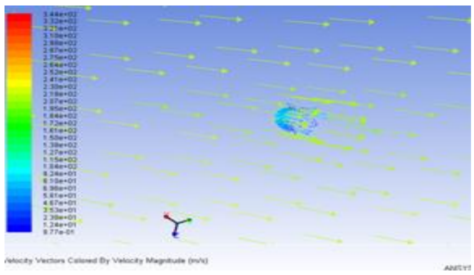

**Figure 15. The velocity vector at the blade**

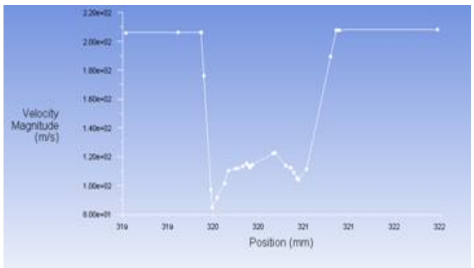


**Figure 16. The velocity curve at the blade pit**

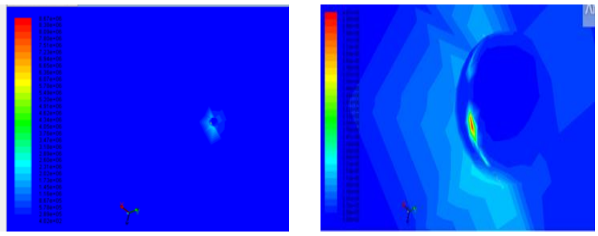

**Figure 17. The Fluid strain rate in corrosion pit of the blade**

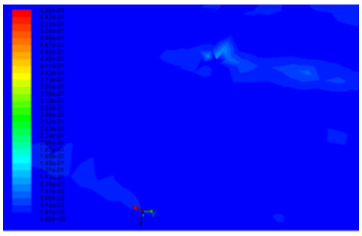

**Figure 18. The sedimentary concentration of Cl⁻ in the corrosion pit of the blade**

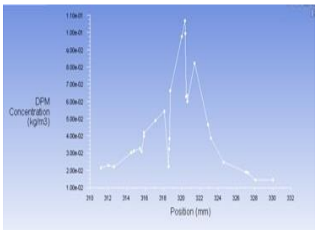

**Figure 19. The sedimentary concentration of $Cl^-$ at the corrosion pit of the blade**

## 5. Conclusion

Based on the computational simulation of blades with pitting corrosion as well as the disk, the change of flow field parameters are made out as follows：

(1) The static pressure increased and dynamic pressure decreased in the upstream face of pitting and the fluid velocity decreased sharply. Vortex backflows appear at the pitting defect.

(2) The flow becomes complicated near the pitting and the blade would be easy to crack with fluid shear rate varying widely and the stress distribution deteriorates under the influence of fluid in the pitting area.

(3) The Cl- concentration is 50 times higher than before in the pitting area where is easily to be the origin of the crack and the phenomenon coincides with stress corrosion test results.

(4) The expanded crack would deteriorate the flow field. Due to such alternates, the appearance of micro-crack would be the safety hazard to the blades. In the actual condition piping natural gas containing $Cl^-$, the results could be used to estimate the expansion of crack originated from the pitting defect that should design with higher safety coefficient.


## Acknowledgement

The work was supported by Shandong Provincial Science and Technology Development Program (2014GGX108001 and 2016GGX104018).

## References


[1] Hou, S. Q., Wang, C. X., Lin, J. Z. (2005) Summary of Numerical Simulation of the Internal Flow in the Turbomachinery. *FLUID MACHINERY*, **5**, 33.

[2] Chen, X., Miao, Y. M. (1992) The computation of internal flow fields in centrifugal compressor impellers. *Journal of Thermos-physics Engineering*, **3**, 13

[3] Hu, S. B., Su, M. M. (2009) Numerical Study on Loading Rules of Centrifugal Compressor Impeller. *Compressor Blower & Fan Technology*, **4**, 25-27.

[4] Liu, X. Z., Cao, S. Z., Gu, C. G. (2000) Computational and Experimental Investigation of 3-D Turbulent Flow Field in Centrifugal Impeller. *FLUID MACHNERY*, **28**(4):9-12.

[5] Yakhot V., Orzag S. A.（1986） Renormalization group analysis of turbulence：basic theory. *Scient Comput*.**1,** 3-11.

[6] Hu, S. B., Su, M. M.. (2010) Comparison of Different Turbulence Model for Numerical Simulation of Internal Flow of Centrifugal Compressor. *FLUID MACHNERY*, **8**, 38

[7] Balje O. E. Turbo-machine A : Guide to Design, Selection and Theory. America: Wiley Inter-science Publication, 1981.

[8] Krain H. (1999) High Pressure Ratio Centrifugal Compressor with Transonic Flow. *Proceeding of the 3rd ASME/ JSME Joint Fluids Engineering Conference*. July 18 -23.

[9] Zhang, L., Chen, H. P., Xu, Z. (2000) Quasi-three Dimensional Iterative Numerical Analysis for Flow Field in Compressor Impellor. *Fan Technology*, **5**, 3-7.

[10] Chen, Q., Zhang, B. Z., Cui, C. L.（2010） Quasi Orthogonal Surface Calculation for Three dimensional Flow in Centrifugal Fan. *Journal of Hangzhou Institute of Application Engineering*, **12**, 21-23.

[11] Epureanu B. I., Hall K. C., Dowell E. H. (2001) Reduced Order Models of Unsteady Viscous Flows in Turbomachinery Using Viscous Inviscid Coupling. *Journal of Fluids and Structures*, **15**, 255-273.

[12]Borello D., Corsini A., Rispoli F. (2003) A finite element overlapping scheme for turbomachinery flows on parallel platforms. *Computers & Fluids*, **32**, 1017-1047.